Morphologic Changes in Acute Central Serous Chorioretinopathy Evaluated by Fourier-Domain Optical Coherence Tomography

Hisataka Fujimoto, MD, Fumi Gomi, MD, PhD, Taku Wakabayashi, MD, Miki Sawa, MD, Motokazu Tsujikawa, MD, Yasuo Tano, MD

Objective: To investigate morphologic alterations around fluorescein leakage sites using Fourier-domain optical coherence tomography (FD OCT) in acute central serous chorioretinopathy (CSC).

Design: Observational case series.

Participants: Twenty-one eyes with acute CSC with subjective symptoms for under 3 months.

Methods: Patients underwent measurement of visual acuity, fundus observations, and FD OCT examinations at every visit with the intervals of 2 to 4 weeks until subretinal fluid (SRF) resolved. Fluorescein angiography was performed at baseline to confirm dye leakage sites. Horizontal and vertical OCT scans (B-scans and consecutive raster scans) of the fovea and fluorescein leakage sites were obtained.

Main Outcome Measures: Morphologic changes in the retinal pigment epithelium (RPE), detached retina, and subretinal space around the leakage sites were evaluated repeatedly during follow-up.

Results: The mean period between baseline and the final examination was 108 days (mean no. of examinations, 3.9). Among 23 leakage sites in 21 eyes, FD OCT showed RPE abnormalities in 22 (96%) sites (14 sites [61%] with a pigment epithelial detachment [PED] and 8 [35%] with a protruding or irregular RPE layer). Fibrinous exudates in the subretinal space and sagging/dipping of the posterior layer of the neurosensory retina above the leakage sites were seen at 12 (52%) and 10 (43%) leakage points, respectively. An RPE defect at the edge of or within the PED was observed in 5 leakage sites (22%); in 2 of these, a defect was detectable after the SRF decreased. The posterior surface of the detached retina was smooth in 17 eyes (81%) and granulated in 4 eyes (19%) (mean duration of subjective symptoms, 10 days and 42 days, respectively). The smooth posterior detached retina became granulated in the presence of residual SRF. A PED remained at the 5 leakage sites in 5 eyes (22%) despite SRF resolution.

Conclusions: Fourier-domain OCT examinations showed detailed morphologic changes in eyes with acute CSC including an RPE defect within the PED at a leakage site through which fluid might pass from the sub-RPE to the subretinal area. Fourier-domain OCT findings may offer new information to facilitate understanding of the mechanisms of acute CSC.

Financial Disclosure(s): Proprietary or commercial disclosure may be found after the references. *Ophthalmology 2008;115:1494–1500 © 2008 by the American Academy of Ophthalmology.*

Eyes with acute central serous chorioretinopathy (CSC) have focal leakage at the level of the retinal pigment epithelium (RPE) seen on fluorescein angiography (FA).[1,2] Evaluations using indocyanine green angiography in eyes with CSC have shown multifocal islands of inner choroidal staining; therefore, the exudative changes within the inner choroid are considered to be the primary event in the disease.[3–7] The subsequent changes at the RPE allow the fluid to enter the subretinal space, and those changes are thought to be reversible because spontaneous resolution of the subretinal fluid (SRF) is not uncommon. However, except for FA findings, the detailed features of the RPE abnormalities have not been documented during development and resolution of the SRF.

Morphologic changes in eyes with CSC have been reported using optical coherence tomography (OCT).[8–18] This imaging technology records the various features of CSC, including retinal detachment (RD), fibrinous exudation, and cystic changes within the retina. To detect the RPE changes corresponding precisely to the leakage points on FA, we evaluated en face images of OCT and frequently observed minute pigment epithelial detachments (PEDs) or RPE protrusions.[15] However, these abnormalities cannot explain the fluid migration from the choroidal space to the subretinal space.

Recently, a Fourier-domain (FD) OCT system was introduced for the advanced ophthalmic imaging[19–25] that reduces the image acquisition time and allows the entire area of interest to be imaged on a detailed retinal structural map. In the currently available commercial FD OCT unit, C-scans (en face images) can be reconstructed from the set

of B-scan volume data, and the C-scan images can be combined in Z directions. This enables us to compose a scanning laser ophthalmoscope–like fundus image. These nearly simultaneous multiple perspective views can be used to define the locations of the lesions clearly.

In the current study, we examined the FD OCT images from patients with CSC in the acute and active forms to evaluate the use of rapid scanning to gain a better understanding of the morphologic changes in this disease.

Materials and Methods

We prospectively studied 21 eyes of consecutive 20 patients (18 men, 2 women) with acute CSC using the FD OCT system (RTVue-100, Optovue, Fremont, CA) between June 2006 and May 2007 at Osaka University Medical School, Osaka, Japan. This study was approved by the institutional review board, and informed consent was obtained from all patients.

A diagnosis of acute CSC was made based on the presence of a serous detachment of the neurosensory retina, focal dye leakage on FA, and the duration of recent subjective symptoms within 3 months. Polypoidal choroidal vasculopathy, which is sometimes difficult to differentiate from CSC by FA, was excluded by the absence of polypoidal choroidal vascular lesions on indocyanine green angiography. Eyes with other macular abnormalities such as neovascular maculopathy also were excluded.

A fundus examination, measurement of the best-corrected visual acuity (BCVA), and FD OCT imaging were performed at every visit. Fluorescein and indocyanine green angiography were performed using a fundus camera (TRC 50EX/ImageNet, Topcon,
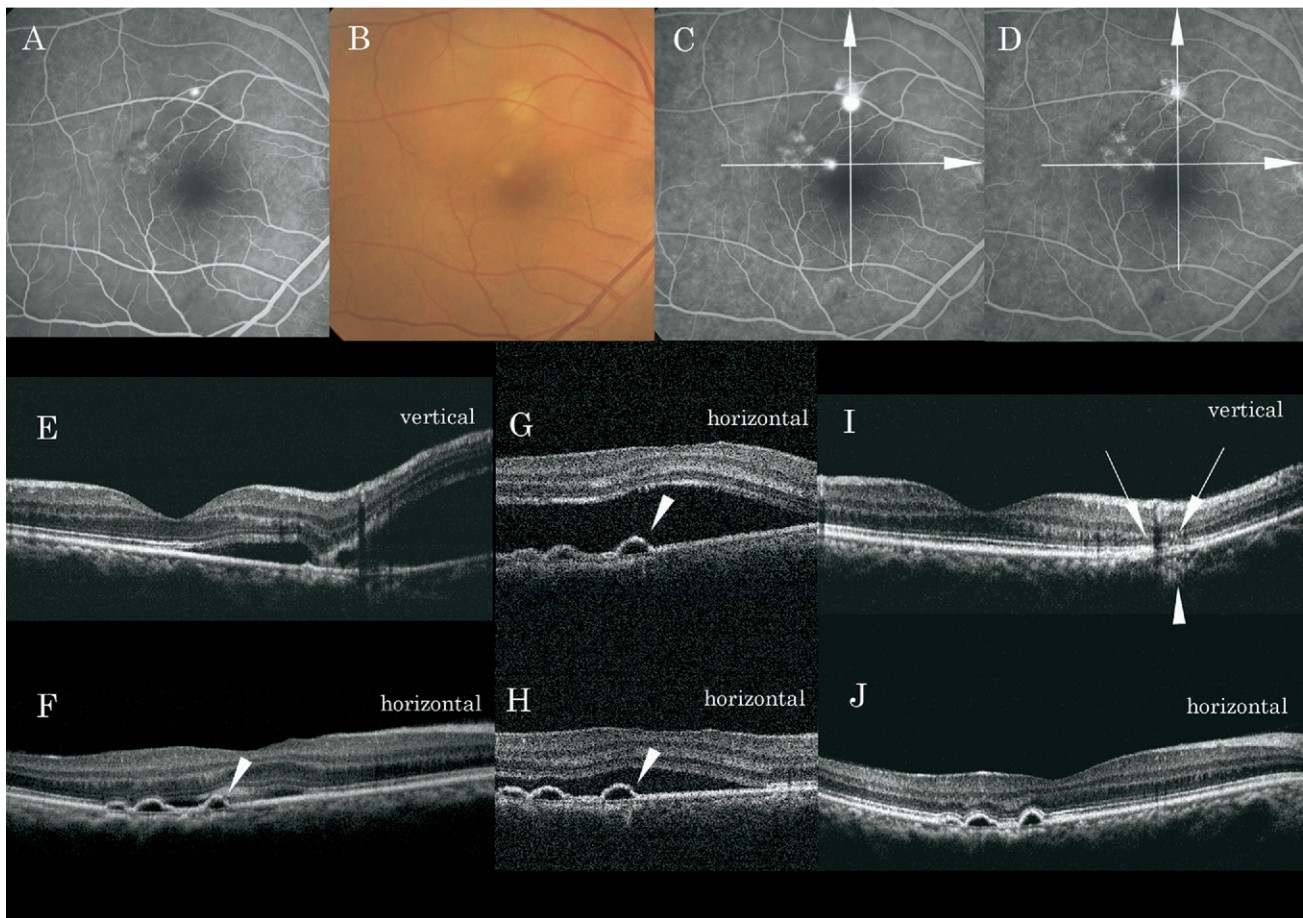

Figure 1. Findings from a 39-year-old man (patient 19) with acute central serous chorioretinopathy (CSC). **A,** Fluorescein angiography (FA) from a CSC episode 1.5 years previously shows a leakage site outside of the upper vascular arcade and multiple hyperfluorescent lesions temporal to the fovea. The leakage was treated by laser. **B,** The CSC recurred; a fundus photograph shows subretinal fluid (SRF) with 2 regions of white exudates. **C,** An FA image depicts 2 leakage sites, one just under the previous leakage site and one being a dotlike hyperfluorescence near the fovea on a previous FA image. Only the upper leakage site was treated by laser 2 weeks after, and the SRF resolved. **D,** An FA image 2 months after treatment shows multiple hyperfluorescent regions without leakage. **E,** The vertical Fourier-domain optical coherence tomography (FD OCT) image corresponding to the vertical arrow in C shows the retina dipping above the irregular retinal pigment epithelium (RPE) with slight fibrin. **F,** A horizontal FD OCT image corresponding to the horizontal arrow in C shows 3 pigment epithelial detachments (PEDs), one of which is accompanied by fibrinous exudates. An RPE defect is seen in the leaking PED (arrowhead). **G,** A horizontal image from raster scans 2 weeks after the initial examination also shows an RPE defect (arrowhead) and increased SRF. **H,** Two weeks after the laser to the upper leakage site, the SRF is decreasing, but an RPE defect (arrowhead) is still visible. Two months after the laser treatment, the vertical (**I**) and horizontal (**J**) FD OCT images corresponding to the arrows in D show resolution of the SRF. **I,** Focal disruption of the photoreceptor inner and outer segments (arrows) and abnormal signals beneath the RPE (arrowhead) probably correspond to the region of previous and current laser treatments. **J,** Although 3 PEDs remain, no RPE defect is seen.

Tokyo, Japan) at least at baseline. Patients were observed without intervention for 2 to 4 weeks, and then thermal photocoagulation was proposed for cases in which the SRF remained. Follow-up was continued at least until the complete resolution of the SRF was confirmed by FD OCT with intervals of 2 to 4 weeks.

Analysis by FD OCT was performed using cross scans with an 8-mm range and 3-dimensional raster scans using the RTVue system. The light source of the RTVue is an 840-nm superluminescent diode with a 50-nm-spectrum bandwidth. The system uses a grating-based FD method, so it can achieve an ultrahigh scan speed of 26 000 A-scans per second. The transverse and depth resolution claimed by manufacturer is 15 μm and 5 μm, respectively. The A-scan depth is 2 mm for retina scan. The cross scans are a pair of 1024 A-scans/frame B-scans oriented horizontally and vertically. Multiple scans are processed and averaged to reduce the speckle noise. The 3-dimensional raster scan consists of 101 frame B-scans equally spaced in a rectangular area 4×4×2 mm (lateral×lateral×depth). Each B scan is 512 A-scans/frame. The scan time for a 3-dimensional raster scan is 2 seconds.

In the current study, the morphologic changes in the retina and RPE in eyes with acute CSC were analyzed using FD OCT images, especially around the fluorescein leakage site. Because the 3-dimensional raster scan of the RTVue system can display a composed fundus image by adding up the enface C-scan images in Z directions, this fundus image was used to register the location, and the FA image was superimposed on this projected fundus image to determine the corresponded B-scan image around the leakage site. The labeling of the layer in the outer retina on the acquired FD OCT images was done based on the previous reports.[24,25]

Results

Patient Characteristics

The profiles of the patients are shown in Table 1 (available at http://aaojournal.org). The mean age of the 20 patients was 47.4 years (range, 32–65). The duration of symptoms ranged from 1 to 86 days (mean, 16.0). Four eyes had recurrent disease, and the other 2 had CSC history in the fellow eye. The mean BCVA at baseline was 0.84 (range, 0.2–1.5). Nineteen eyes had 1 point of focal leakage and 2 eyes showed 2 points of leakage; 17 leakage points in 16 eyes (74%) had an inkblot pattern, and 6 leakage sites in 5 eyes (26%) showed a smokestack pattern. The indocyanine green angiography showed increased hyperfluorescence of the choroidal vein around the leakage site in all eyes.

The mean period between baseline and the time of confirmation of complete resolution of the SRF was 65 days (range, 28–155),

Figure 2. A 65-year-old man (patient 17) with a 5-day history of visual deterioration shows intense leakage with a smokestack pattern on early-phase and midphase (**A, B**) fluorescein angiography (FA). **C,** The Fourier-domain optical coherence tomography (FD OCT) image (vertical section corresponds to the arrow in B) shows a thin stringlike subretinal structure (arrow) bridging the neurosensory retina and pigment epithelial detachment (PED). A defect in the retinal pigment epithelium (RPE) on PED is suspected, but there is the possibility that this is an artifact. Four weeks after the initial examination, the subretinal fluid decreased spontaneously, and early-phase and midphase FA (**D, E**) shows a marked decrease in leakage. **F,** The FD OCT images (corresponding to the horizontal line in E) reveal a defect in the RPE at the top of the PED (arrowhead), which seems exactly at the dye leakage site. A high OCT signal in the choroid seems to be derived from lack of light absorption by the RPE. **G–I,** A defect in the RPE (arrowhead) is seen in 2 successive 3-dimensional sections of 40-μm intervals.
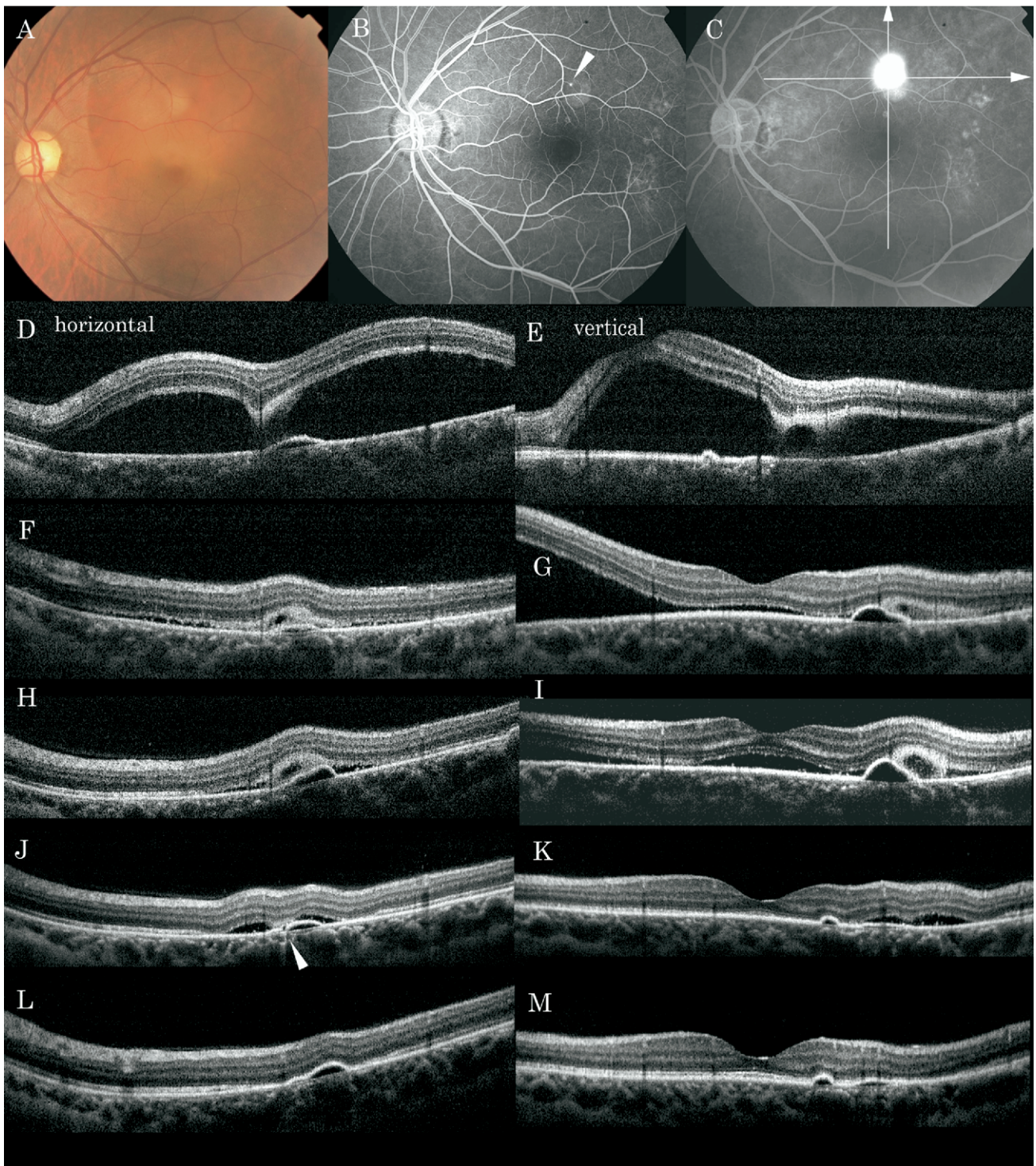
Figure 3. A 42-year-old man (patient 16) showed subretinal fluid (SRF) with yellow–white exudate on the fundus (**A**) and intense dye leakage resembling an inkblot on early-phase and midphase fluorescein angiography (FA) (**B, C**). The left panels of the images from Fourier-domain optical coherence tomography correspond to the horizontal line on C including the leakage site. The right panels show vertical images on C including the macula and leakage site. **D, E**, At the initial examination, extensive SRF is present involving the macula. A pigment epithelial detachment (PED), retinal dipping, and fibrinous exudation with a translucent lesion are seen at the leakage site. **F, G**, Two weeks later, the SRF has decreased around the leakage site and shifted inferiorly. The patient did not agree to undergo laser treatment. **H, I**, Four additional weeks later, the SRF remains around the macula and leakage site. The posterior surface of the detached retina became thin and granular at the macula, and fibrinous exudates around the leakage site are seen as a white mass on the fundus examination. **J, K**, Four weeks later, the SRF is detected around the leakage site, and a defect of the RPE layer (arrowhead) is observed. A retinal reattachment is seen around the macula without the appearance of photoreceptor inner and outer segments (IS/OS). The laser was administrated to avoid the recurrence because the residual leakage was seen on FA. **L, M**, Two weeks later, complete retinal reattachment has occurred, although the PEDs remain. The IS/OS line is seen in the macula.
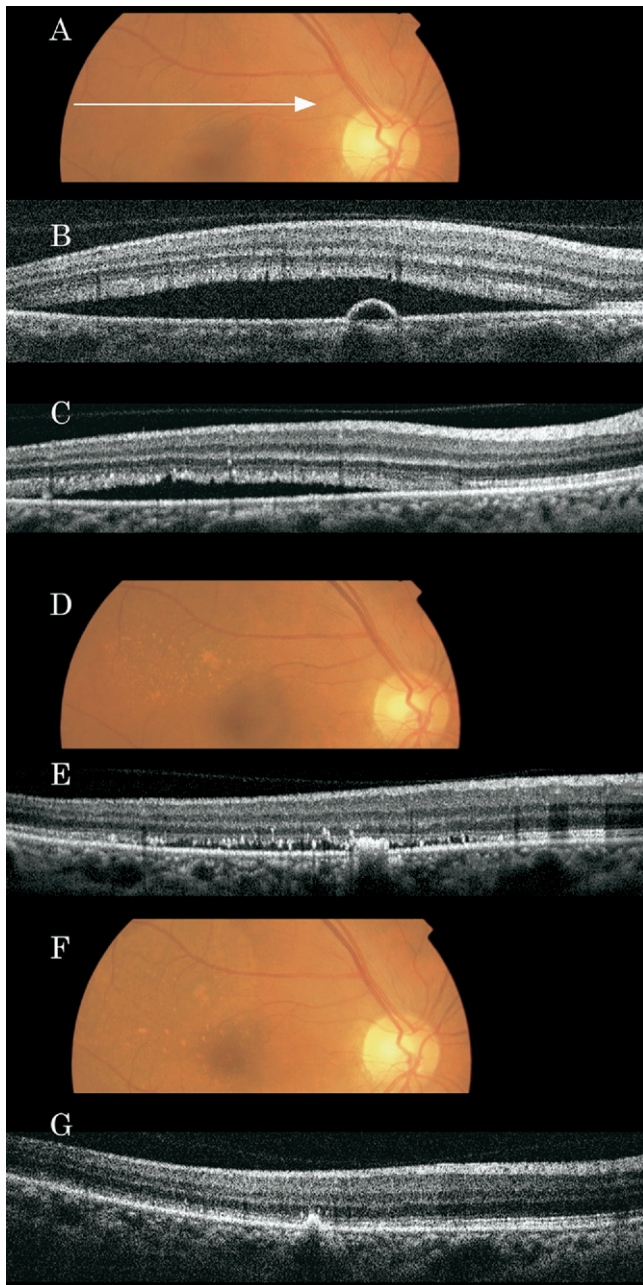
Figure 4. Images from a 56-year-old woman (patient 13). A Fourier-domain optical coherence tomography (FD OCT) image 3 weeks after onset of central serious chorioretinopathy corresponding to the arrow on the fundus image (**A**) shows subretinal fluid (SRF), a smooth and thick outer photoreceptor layer, and a pigment epithelial detachment (PED) at the dye leakage site (**B**). **C**, An FD OCT image 3 weeks after the previous examination and 1 week after thermal photocoagulation shows that the photoreceptor outer segment has become granulated, with reduced thickness. A funduscopic image obtained 5 weeks after the initial examination shows white discrete precipitates and their aggregated products (**D**), and the FD OCT image shows scattered and aggregated subretinal precipitates (**E**). Two months after the initial examination, those precipitates have gradually decreased on fundus (**F**) and FD OCT (**G**) images, along with the regression of the SRF.

and the mean total follow-up period was 108 days (range, 28–197). Mean number of the examination during the corresponding period were 3.4 and 3.9, respectively. Thermal laser photocoagulation was performed in 13 of 21 eyes (14/23 leakage sites). At the final examination, mean visual acuity (VA) was 1.1 (range, 0.9–1.5).

Fourier-Domain Optical Coherence Tomography Findings at Baseline

At the initial FD OCT examination, a detachment of the neurosensory retina was confirmed in all patients. Among total 23 leakage sites in 21 eyes, 14 points (61%) showed retinal PED within or at the edge of the RD (Figs 1–4), and 8 regions (35%) without an apparent PED showed an irregular RPE layer including a small RPE protrusion (Fig 1); therefore, 22 of 23 leakage sites (96%) had abnormalities of the RPE layer on FD OCT. The size or height of the RPE elevation was unrelated to the disease intensity, speed or extent of dye leakage, or amount of SRF. Minute defects in the RPE layer within the PED were observed in 3 leakage sites and those defects exactly corresponded to the leakage points. The irregularly protruded RPE layer was also observed at different regions from the leakage site in 9 eyes (43%). Of 4 eyes with a history of CSC, 3 treated with laser had an irregular RPE layer with slight disruption of the photoreceptor layer and a faint reflection beneath the RPE, and 1 had a residual PED at the previous leakage points.

In 12 of 23 leakage sites (52%), a hyperreflective shadow suggesting fibrin in the subretinal space was observed around the leakage point (Figs 1, 3). The eyes showed intense subretinal reflectivity accompanied by clinically observed yellow–white subretinal exudation. A translucent area within the shadow was observed in 8 of the 11 leakage sites (Figs 1, 3). Two eyes had a thin stringlike tissue connecting the posterior layer of the neurosensory retina and the PED (Fig 2). In 10 leakage sites (43%), sagging or dipping of the posterior layer of the neurosensory retina, which seemed to arise from the swelling of the outer nuclear layer and be attracted by fibrinous exudates to the protruded RPE at the leakage site, was observed (Figs 1, 3).

The posterior surface of the detached retina had a smooth appearance with increased thickness of the photoreceptor outer segment in 17 eyes (81%) and a granulated appearance in 4 eyes (19%), with mean durations of subjective symptoms of 10 days and 42 days, respectively.

Changes in the Fourier-Domain Optical Coherence Tomography Findings during Follow-up

A defect in the RPE layer within the PED was observed in 2 other eyes as the SRF decreased (Figs 2, 3). In 1 eye, a defect in the RPE was seen in 2 consecutive images from raster scans with 40-μm intervals (Fig 2). Therefore, the diameter of the defect in this eye would be at least 40 μm and <80 μm, although it was the only case in which the RPE defect was seen in consecutive raster scans. Fourteen leakage sites, including 4 with an apparent RPE defect, were treated with laser. At the final examination, complete resolution of the SRF was confirmed in all eyes, although PED remained at the 5 leakage sites (22%).

As to the findings of the posterior surface of the detached retina, a smooth posterior surface at baseline changed to have a granular appearance in 12 of 17 eyes with reduced thickness of the photoreceptor outer segment in the presence of residual SRF (Fig 3). The granulated appearance was more prominent in eyes with white punctate deposits of the fundus, and aggregated granules in the subretinal space seemed to correspond to the white deposits (Fig 4). In no case did the granulated appearance of the photore-

ceptor outer segment become smooth. When the neurosensory retina was attached, the subretinal granules and the white deposits on the fundus began to disappear (Fig 4). Fibrinous exudation remained in the subretinal space for a while after the retina reattached (Fig 3). The line probably corresponded to the junction of the photoreceptor inner and outer segments (IS/OS), which was invisible in the detached retina and became apparent after the fluid resolved (Fig 3). The VA did not appear to correlate with the presence of irregularities of the IS/OS at the fovea.

Discussion

The primary pathology of acute CSC is thought to begin with disruption of the choroidal circulation. The RPE then decompensates and allows exudation from the choroidal vasculature to pass into the subretinal space.[1–7] These hypotheses are based on FA and indocyanine green angiography findings, and precise morphologic correlations have not been observed.

The development of OCT has provided a better understanding of the mechanism in CSC, especially the abnormalities in the RPE layer.[10–12,15–17] We reported the findings on 3-dimensional OCT images of CSC using the OCT-Ophthalmoscope C7 (Nidek, Gamagori, Japan) and detected RPE abnormalities such as a PED, at the leakage points on FA in 26 of 27 eyes (96%).[15] Hirami et al reported that these RPE abnormalities were within areas of choroidal vascular hyperpermeability.[17] However, the initial point of leakage on FA often is a pinpoint and is smaller than a PED or RPE protrusion. Therefore, there might be a defect in the RPE layer that allows passage of fluid from the sub-RPE to the subretinal area, although conventional OCT has not documented such a defect.

In the current study, we observed RPE abnormalities in 95% of eyes with acute CSC and clearly visualized a minute defect of the RPE within the PED, which seemed to correspond precisely to the leakage point on FA in 5 eyes (24%). The absence of RPE at the leakage point is supported by recent findings of fundus autofluorescence. In acute CSC, focal areas of hypoautofluorescence corresponding to the site of the focal RPE leak were observed, and the authors speculated that the origin of the hypoautofluorescence may be blowout of the RPE (corresponding to our minute defect) at or near the junction of the attached and detached RPE.[26] However, not all eyes with CSC had hypoautofluorescence at the leakage site.[27] We observed that only 1 eye had an RPE defect on 2 consecutive raster scans; however, in another 4 eyes a defect was seen in one image from raster scans. Therefore, a defect usually is too small to be detected even by FD OCT or fundus autofluorescence analysis even if all eyes with acute CSC have an RPE defect at the leakage site.

Direct observation of an RPE defect also helps in understanding the fluid dynamics in CSC. If the fluid passes through the defect of RPE that we observed, the resolution of the SRF results from restoration of the defect, decreased effusion from the choroidal vasculature, or both. Repeated FD OCT examinations could show that the SRF may reduce even if the RPE defect is not completely sealed, which indicates the importance of the reduction of the effusion from the choroid. The reduction of the choroidal effusion

may promote a spontaneous closure of an RPE defect. On the other hand, a PED at the leakage site persisted in 22% of eyes after complete resolution of the SRF without any findings of RPE defects, which supports the importance of the restoration of the defect and maintenance of RPE integrity against the increased pressure from the choroid. When the pressure is excessive, a defect of RPE may recur to pass the fluid. Irregular RPE observed at different regions in half of the examined eyes may become the new leakage site if a defect occurs in those abnormal RPE regions. In conclusion, the self-limiting but occasionally recurring nature of acute CSC might be explained by both the RPE integrity and the hydrostatic pressure of the choroid.

The microstructural morphology of the detached retina also showed interesting findings. When the retina detached, the appearance of the outer retinal layer changed; the external limiting membrane persisted, although the IS/OS could not be detected in all eyes, as recently reported by Ojima et al.[25] In the acute phase, the thickness of the probable photoreceptor outer segment increased in the entire area of the detached retina. The increased thickness of the photoreceptor outer segment in the detached retina then gradually decreased, and the outer segment's appearance changed to granular until the reattachment. Previous reports showed punctuate or granular areas in the photoreceptor outer segment more frequently in cases of chronic or recurrent versus acute CSC[14, 25]; however, our findings indicated that when the RD persisted for several weeks, the outer segment developed a granular appearance, probably due to the accumulation of the shed outer segments. After retinal reattachment, the IS/OS gradually become clear, which implies normalization of the assembly of the photoreceptor outer segment by regular phagocytosis by the RPE.

Although histopathologic studies of CSC are limited, FD OCT showed the precise morphologic changes in acute CSC. We showed the presence of a minute RPE defect through which the choroidal exudation leaks into the subretinal space. The findings obtained during the self-limited course of CSC indicate certain mechanisms of the fluid dynamics. Further improvement in this instrument will provide a better understanding of CSC pathology.

References

1. Gass JDM. Stereoscopic Atlas of Macular Diseases: Diagnosis and Treatment. 4th ed. vol. 1. St. Louis, MO: Mosby; 1997: 52–70.
2. Spaide RF. Central serous chorioretinopathy. In: Holz FG, Spaide RF, eds. Medical Retina. Berlin: Springer; 2005:77–93. Essentials in Ophthalmology. Krieglstein GK, Weinreb RN, series eds.
3. Guyer DR, Yannuzzi LA, Slakter JS, et al. Digital indocyanine green videoangiography of central serous chorioretinopathy. Arch Ophthalmol 1994;112:1057–62.
4. Piccolino FC, Borgia L. Central serous chorioretinopathy and indocyanine green angiography. Retina 1994;14:231–42.
5. Scheider A, Nasemann JE, Lund OE. Fluorescein and indocyanine green angiographies of central serous choriodopathy by scanning laser ophthalmoscopy. Am J Ophthalmol 1993; 115:50–6.

6. Prunte C, Flammer AJ. Choroidal capillary and venous congestion in central serous chorioretinopathy. Am J Ophthalmol 1996;121:26–34.
7. Iida T, Kishi S, Hagimura N, Shimizu K. Persistent and bilateral choroidal vascular abnormalities in central serous chorioretinopathy. Retina 1999;19:508–12.
8. Hee MR, Puliafito CA, Wong C, et al. Optical coherence tomography of central serous chorioretinopathy. Am J Ophthalmol 1995;120:65–74.
9. Iida T, Hagimura N, Sato T, Kishi S. Evaluation of central serous chorioretinopathy with optical coherence tomography. Am J Ophthalmol 2000;129:16–20.
10. Kamppeter B, Jonas JB. Central serous chorioretinopathy imaged by optical coherence tomography. Arch Ophthalmol 2003;121:742–3.
11. Montero JA, Ruiz-Moreno JM. Optical coherence tomography characterisation of idiopathic central serous chorioretinopathy. Br J Ophthalmol 2005;89:562–4.
12. van Velthoven ME, Verbraak FD, Garcia PM, et al. Evaluation of central serous retinopathy with en face optical coherence tomography. Br J Ophthalmol 2005;89:1483–8.
13. Saito M, Iida T, Kishi S. Ring-shaped subretinal fibrinous exudate in central serous chorioretinopathy. Jpn J Ophthalmol 2005;49:516–9.
14. Piccolino FC, de la Longrais RR, Ravera G, et al. The foveal photoreceptor layer and visual acuity loss in central serous chorioretinopathy. Am J Ophthalmol 2005;139:87–99.
15. Mitarai K, Gomi F, Tano Y. Three-dimensional optical coherence tomographic findings in central serous chorioretinopathy. Graefes Arch Clin Exp Ophthalmol 2006;244:1415–20.
16. Hussain N, Baskar A, Ram LM, Das T. Optical coherence tomographic pattern of fluorescein angiographic leakage site in acute central serous chorioretinopathy. Clin Experiment Ophthalmol 2006;34:137–40.
17. Hirami Y, Tsujikawa A, Sasahara M, et al. Alterations of retinal pigment epithelium in central serous chorioretinopathy. Clin Experiment Ophthalmol 2007;35:225–30.
18. Shukla D, Aiello LP, Kolluru C, et al. Relation of optical coherence tomography and unusual angiographic leakage patterns in central serous chorioretinopathy. Eye 2008;22:592–6.
19. Wojtkowski M, Bajraszewski T, Gorczynska I, et al. Ophthalmic imaging by spectral optical coherence tomography. Am J Ophthalmol 2004;138:412–9.
20. Wojtkowski M, Srinivasan V, Fujimoto JG, et al. Three-dimensional retinal imaging with high-speed ultrahigh-resolution optical coherence tomography. Ophthalmology 2005;112:1734–46.
21. Chen TC, Cense B, Pierce MC, et al. Spectral domain optical coherence tomography: ultra-high speed, ultra-high resolution ophthalmic imaging. Arch Ophthalmol 2005;123:1715–20.
22. Jiao S, Knighton R, Huang X, et al. Simultaneous acquisition of sectional and fundus ophthalmic images with spectral-domain optical coherence tomography. Opt Express [serial online] 2005;13:444-52. Available at: http://www.opticsexpress.org/abstract.cfm?id=82381. Accessed January 22, 2008.
23. Alam S, Zawadzki RJ, Choi S, et al. Clinical application of rapid serial Fourier-domain optical coherence tomography for macular imaging. Ophthalmology 2006;113:1425–31.
24. Hangai M, Ojima Y, Gotoh N, et al. Three-dimensional imaging of macular holes with high-speed optical coherence tomography. Ophthalmology 2007;114:763–73.
25. Ojima Y, Hangai M, Sasahara M, et al. Three-dimensional imaging of the foveal photoreceptor layer in central serous chorioretinopathy using high-speed optical coherence tomography. Ophthalmology 2007;114:2197–207.
26. Eandi CM, Ober M, Iranmanesh R, et al. Acute central serous chorioretinopathy and fundus autofluorescence. Retina 2005;25:989–93.
27. von Ruckmann A, Fitzke FW, Fan J, et al. Abnormalities of fundus autofluorescence in central serous retinopathy. Am J Ophthalmol 2002;133:780–6.

Footnotes and Financial Disclosures

Correspondence:
Fumi Gomi, MD, PhD, Department of Ophthalmology, Osaka University, Graduate School of Medicine, Room E7, 2-2 Yamadaoka Suita, Osaka, Japan. E-mail: fgomi@ophthal.med.osaka-u.ac.jp.

Table 1. Clinical and Optical Coherence Tomography Characteristics of Patients with Acute Central Serous Chorioretinopathy

Case/Gender	Age	History	Symptom Duration (Days)	FA Leakage Sites/Leakage Pattern
1/M	54		2	1/inkblot
2/F	56		17	1/inkblot
3/M	55	2.5 yrs prior	7	1/inkblot
4/M	33		3	1/inkblot
5/M	49		8	1/inkblot
6/M	45		5	1/inkblot
7/M	39		9	1/inkblot
8/M	46		14	1/smokestack
			28	1/inkblot
9/M	60		5	1/inkblot
10/M	36	2.5, 0.5 years prior	21	2/smokestacks
11/M	43	2 yrs prior	25	1/smokestack
12/M	54		8	1/inkblot
13/F	56		12	1/inkblot
14/M	53		9	1/inkblot
15/M	49		30	1/inkblot
16/M	42		10	1/inkblot
17/M	64		5	1/smokestack
18M	53		86	1/ink blot
19M	39	1.5 yrs prior	9	2/inkblots
20/M	41		42	1/inkblot

F = female; FA = fluorescein angiography; FD OCT = Fourier domain optical coherence tomography; M = male; PED = pigment epithelial detachment; RPE = retinal pigment epithelium; VA = visual acuity.

Table 1. Continued

				FD OCT Findings					
Findings at Leakage Point	RPE Defect	Irregular RPE except Leakage Site	Sagging/Dipping of Posterior Neurosensory Retina Layer	Hyperreflective Shadow in Subretinal Space	Changes in Back Surface of Detached Retina	Residual PED at Last Visit	Laser	Follow-up (Days)	Initial and Final VA
PED		No	Yes	Yes	Smooth→granulated→attached	Yes		197	0.9, 1.0
PED		Yes	No	No	Smooth→smooth→attached	No	Yes	109	1.2, 1.2
PED		No	No	No	Smooth→granulated→attached	Yes		140	0.7, 0.8
Irregular RPE		No	Yes	No	Smooth→granulated→attached	—		118	1.5, 1.5
PED	Yes	No	Yes	Yes	Smooth→attached→attached	No	Yes	84	0.3, 1.2
PED		No	Yes	Yes	Smooth→granulated→attached	No		60	0.2, 1.2
Irregular RPE		No	No	No	Smooth→granulated→attached	—	Yes	128	1.0, 1.2
Irregular RPE		Yes	No	No	Smooth→granulated→attached	—		88	1.2, 1.2
PED		Yes	No	No	Granulated→granulated→attached	No	Yes	90	0.6, 0.8
PED		Yes	Yes	No	Smooth→granulated→attached	No		186	0.8, 1.2
Irregular RPEs		Yes	Yes	Yes	Smooth→attached→attached	—		45	1.5, 1.2
Irregular RPE		No	No	No	Granulated→granulated→attached	—	Yes	142	1.0, 1.0
Irregular RPE		No	No	No	Smooth→granulated→attached	No	Yes	82	1.2, 1.2
No		No	No	No	Smooth→granulated→attached	—	Yes	122	0.8, 1.2
PED		Yes	No	No	Smooth→granulated→attached	Yes		86	1.2, 1.2
PED	Yes	No	No	Yes	Smooth→granulated→attached	No	Yes	28	1.0, 1.2
PED	Yes	Yes	Yes	Yes	Smooth→granulated→attached	Yes	Yes	174	0.9, 1.2
PED	Yes	Yes	Yes	Yes	Smooth→granulated→attached	No	Yes	152	0.6, 0.9
PED		No	No	Yes	Granulated→attached	No	Yes	70	1.0, 1.0
PED, irregular RPE	Yes	Yes	Yes	Yes	Smooth→attached	Yes	Yes	90	0.9, 1.2
PED		No	No	Yes	Granulated→granulated→attached	No	Yes	84	0.7, 1.0